

Responsive PNIPAM coated Au core-shell nanoparticle for optical sensing

S. Faujdar¹, P. Pathania^{2*}, A. Preet², J. Katyal¹

¹ Department of Physics, Amity Institute of Applied Science, Amity University, Noida 201301, India

² Department of Applied Sciences, Galgotias College of Engineering and Technology, Greater Noida, 201306, India

Received: April 15, 2023; Revised: July 25, 2023

In this work, we analyze the optical properties of responsive poly (N-isopropylacrylamide) (PNIPAM) coated plasmonic Au core-shell nanoparticle for sensing application. With external chemical or physical stimuli, the responsive PNIPAM polymeric layer exhibits unique properties like variation of solvent concentration, density and subsequently a change in refractive index (RI). Mie theory-based calculation modeled the change in the position of the localized surface plasmon resonance (LSPR) peak with linear change in refractive index of PNIPAM-coated Au nanosystem with external stimuli like change in salt concentration in water, temperature, pH, etc. It paves the way for designing efficient PNIPAM-coated Au-based refractive index-based system for bio/chemical sensing/detection. We theoretically report the sensitivity (S) equal to ~ 65.8 nm/RIU and the corresponding figure of merit (RIU/nm) is $\sim 3.6 \times 10^2$ RIU/nm. Present investigation can lead to the realization of efficient bio/chemical sensors and light harvesting structures/devices.

Keywords: Plasmonics; Surface Plasmon; Sensor; PNIPAM; Core-Shell Nanoparticle;

INTRODUCTION

Sub-wavelength light-matter interaction and corresponding plasmonic excitation has unfolded new and interesting avenues for advanced research due to formation of localized surface plasmons in metallic nanoparticles [1]. Nanosystems based on plasmonic nanoparticles possess the potential of achieving subwave length confinement below diffraction limit [2-4]. It can subsequently lead to the realization of ultrasensitive bio/chemical sensors, medical diagnostics, metamaterials, imaging, spectroscopy, lensing, lasing, fast optical switches, highly coherent nanolasers [5-10], etc. The key properties of nanoparticle-based plasmonic systems like resonant wavelength, scattering efficiency, absorption efficiency, and electric field/ intensity enhancement can be controlled through size, shape and material of nanoparticles [11]. The optical response of nanoparticles-based plasmonic system is mainly characterized by: (I) dielectric function, (II) the spectral range in which LSPRs can be excited, (III) peak value and FWHM of resonance. Conventionally, noble metals (e.g., silver, gold, aluminum, copper, etc.) have been the primary and most widely employed plasmonic materials for plasmonic-based systems and components operating in visible and IR region [11]. Due to the substantial progress in synthesis, designing, and characterization tools for concentric core-shell nanoparticles, these particles are being widely investigated and finding diverse applications. The

polarization-independent tunable core shell nanoparticle system which consists of the core and shell/cladding geometry, has the innate capacity to fine-tune the resonance peak's spectral characteristics through altering the relative sizes of the core and shell [12]. Owing to the better tunability of resonance wavelength, and controllability of optical properties, core-shells have found applications in SERS, refractive index-based sensing, optical switching, lasing, etc. This shows that plasmonic nanostructures and systems contain the core-shell nanoparticle as a crucial component for bio-molecular sensing [13]. In recent years, unique optical properties of gold-coated responsive polymer hybrid plasmonic-based systems, play an important role in engineering of photonic materials and plasmonic (active) metamaterials in a variety of applications, including sensing, detection, plasmon-enhanced optical spectroscopic readout, etc. [14, 15]. Gold-coated 8-nm thick responsive polyaniline (PANI) shell exhibits plasmon resonance peak wavelength shift by 107 nm due to modulation of refractive index at the interface of core (gold)-shell (polymer) system [16]. Wu and coworkers investigated a PNIPAM shell (thickness=2.6 nm) - coated core gold nanoparticle (diameter =14.8 nm) for "calorimetric temperature sensor and temperature switchable catalyst" [17]. Miller and Lazarides demonstrated the LSPR peak position's sensitivity for Au nanoparticles and core shell of various shapes and sizes with variations in the

* To whom all correspondence should be sent:
E-mail: pathania.p@gmail.com

refractive index in dielectric environment [18]. The responsive polymer-coated plasmonic nanostructures can change their atomic configuration and subsequently their characteristics in the presence of external stimuli, e.g., pH, ions, temperature, light, electric or magnetic field, or biochemical agents [19-23]. The thermo-responsive polymers are the most frequently used materials for both *in vivo* and *in vitro* bio-medical applications. The responsive polymer-coated Au hybrid nanostructure like core shell, nanocages, nanostar, are used successfully in chemo-photothermal therapy of breast cancer cells, and photochemotherapy of pancreatic cancer with gemcitabine [24, 25]. The chemical synthesis of spherical gold nanoparticles with a diameter of 15 to 50 nm in 100 nm coated thick PNIPAM-based hydrogel shell was used to detune the LSPs on collapse of PNIPAM in dynamic light scattering studies [26]. The most recent developments in the use of such responsive plasmonic nanomaterials are discussed, with a focus on plasmonic bio/chemical sensing which makes use of refractometric measurements, plasmon-enhanced optical spectroscopy readout, optically driven miniature soft actuators, and light-powered micromachines that operate in a setting similar to biological systems [27]. In the literature it is found that the LSPR resonant peak's position varies with the responsive PNIPAM shell characteristics (from swollen to collapsed) due to the surrounding physical and chemical environment. The PNIPAM microgels coupled with gold nanoparticles were used as plasmonic sensor components in a smart wearable device that enables naked-eye reading of temperature changes in contact with skin [28]. LSPs supported by a single metallic nanoparticle can be activated by altering the sensitive hydrogel shell's surrounding refractive index. The local rise in the refractive index caused by the collapse of the hydrogel shell next to the metallic core often causes resonant excitation of LSPs to red-shift to longer wavelengths. It is evident that sensitivity of the LSPR to the dielectric environment grows linearly with the position of the LSPR [21]. We present the Mie theory-based investigation of optical (extinction cross-section) properties of the gold/core-PNIPAM/shell-based plasmonic system. In this work, we investigate and optimize the sensing parameters of Au-coated responsive PNIPAM plasmonic system for sensing/detection.

THEORY

The schematic diagram of the core-shell nanoparticle is shown in Fig. 1 with geometrical

parameter (a) of metal Au core having permittivity ϵ_1 radius R_1 , and polymeric PNIPAM shell having permittivity ϵ_2 and radius R_2 , ingrained in a medium of permittivity ϵ_m . The optical response of nanoparticles is modeled using wavelength-dependent dielectric function of plasmonic Au material. The plasmonic system is exposed to uniform electric field directed along +Z direction.

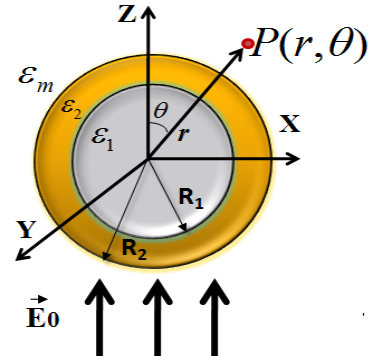


Figure 1. The schematic diagram shows a spherical Au metallic core of radius R_1 with frequency/wavelength dependent dielectric function ϵ_1 covered by polymeric PNIPAM shell of radius R_2 with dielectric function ϵ_2 ingrained in a medium having dielectric constant ϵ_m . The excitation of localized plasmon modes of gold modifies the electric field near the nanoparticle.

The incident electromagnetic waves are expanded in partially spherical waves using vector spherical harmonics. Solving Maxwell's equation and using boundary condition in each layer of core-shell nanoparticle to calculate the Mie coefficients a_l and b_l of the scattered and interior waves is described in the form of Bessel's and Hankel's functions as shown below [29]:

$$a_l = \frac{\psi_l(x_2)[\psi_l'(f_2x_2) - A_l\chi_l'(f_2x_2)] - m_2\psi_l(x_2)[\psi_l(f_2x_2) - A_l\chi_l(f_2x_2)]}{\xi_l(x_2)[\psi_l'(f_2x_2) - A_l\chi_l'(f_2x_2)] - m_2\xi_l'(f_2)[\psi_l(f_2x_2) - A_l\chi_l(f_2x_2)]}$$

$$b_l = \frac{f_2\psi_l(x_2)[\psi_l'(f_2x_2) - B_l\chi_l'(f_2x_2)] - \psi_l(x_2)[\psi_l(f_2x_2) - B_l\chi_l(f_2x_2)]}{f_2\xi_l(x_2)[\psi_l'(f_2x_2) - B_l\chi_l'(f_2x_2)] - \xi_l'(x_2)[\psi_l(f_2x_2) - B_l\chi_l(f_2x_2)]}$$

where the unknown coefficients are:

$$A_l = \frac{f_2\psi_l(f_2x_1)[\psi_l'(f_2x_1)] - f_l[\psi_l'(f_2x_1)\psi_l(f_1x_1)]}{[f_2\chi_l(f_2x_1)\psi_l'(f_1x_1)] - f_l\chi_l'(f_2x_1)\psi_l(f_1x_1)}$$

$$B_l = \frac{f_2\psi_l(f_1x_1)[\psi_l'(f_2x_1)] - f_l[\psi_l'(f_2x_1)\psi_l'(f_1x_1)]}{[f_2\psi_l'(f_2x_1)\psi_l(f_1x_1)] - f_l\psi_l'(f_2x_1)\chi_l(f_2x_1)}$$

where f_1 and f_2 are the relative refractive indices of the core and clad/shell with respect to ingrained medium, $x_1 = kR_1$, $x_2 = kR_2$ are the size parameters.

The Recatti Bessel functions written in terms of Bessel function are:

$$\psi_l(x) = xj_l, \chi_l(x) = -xy_l, \xi_l(x) = xh_l.$$

When the optimized Mie coefficients are known, the extinction efficiency, scattering efficiency, and absorption efficiency of the system are calculated using equation (1) [29]:

$$\left. \begin{aligned} Q_{\text{ext}} &= \frac{2}{x^2} \sum_{l=1}^{\infty} [2l+1] \text{Re}(a_l + b_l) \\ Q_{\text{sca}} &= \frac{2}{x^2} \sum_{l=1}^{\infty} [2l+1] (|a_l|^2 + |b_l|^2) \\ Q_{\text{abs}} &= Q_{\text{ext}} - Q_{\text{sca}} \end{aligned} \right\} \quad (1)$$

In order to validate the present theoretical calculations, we reproduced a result reported in ref. [13] using our developed Matlab code. The calculated extinction cross-section Au-based core-shell [13] nanoparticle of different sizes [($R_1 = 2$ nm, $R_2 = 4$ nm), ($R_1 = 8$ nm, $R_2 = 10$ nm), ($R_1 = 15$ nm, $R_2 = 17$ nm)] embedded in air is presented in Fig. 2. The calculated spectral variation data using Mie theory-based calculations are shown as solid lines and corresponding circles are taken from ref. [12]. An excellent match between present calculations and those published in literature validates our theoretical method (MATLAB code).

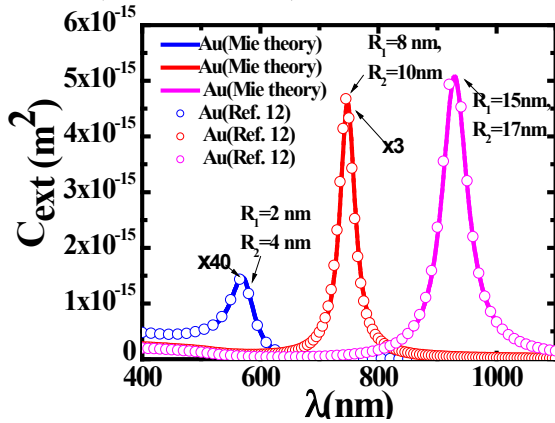


Figure 2. Calculated (solid line) extinction cross-section (C_{ext}) for core (silica)/ shell (gold) nanoparticle based on Mie theory. The results reported in ref. [12] are also shown (open circles) for the validation purpose. The dielectric constant of silica core is $\epsilon_2=2.04$. An excellent match validates the approach used for present investigations.

RESULTS AND DISCUSSION

This section presents the results of theoretical investigations of Au-coated poly (N-isopropylacrylamide) (PNIPAM) core-shell nanoparticle-based nanosystems embedded in water (refractive index 1.33) using Mie theory. The radius

(R_1) of the inner gold core is taken as 5 nm and the thickness of surrounding polymeric shell (R_2) is 2 nm. The refractive index of Au is adopted from Palik's experimentally fitted data [13]. The optimized parameter (χ) models the effective quality of the solvent in the polymer layer which controls the volume fraction and strength of the polymer interaction forces [21]. The film is considered as inhomogeneous only in the radial coordinate. The optimized linear-dependent refractive index of the polymeric shell at 2 nm thickness coated in 5 nm gold core is taken from ref. [21]. The radial-dependent refractive index (n_p) of the polymer layer of thickness 2 nm coated at core Au radius 5 nm is modeled as 1.34 ($\chi = 2.0k_B T$), 1.37 ($\chi = 1.2k_B T$), 1.43 ($\chi = 0.8k_B T$), 1.48 ($\chi = 0.0k_B T$) and at polymer collapse the corresponding refractive index is 1.52 [20]. Au-PNIPAM core shell nanosystem is kept in water as a surrounding medium having refractive index of 1.33. The change in external stimuli like temperature, pH, salt concentration, etc., leads to a change in χ from good solvent ($\chi = 0 k_B T$) to poor solvent ($\chi = 2 k_B T$) responsible for polymer collapse, corresponding to an increase in the average polymer volume fraction with decrease in film thickness. The calculated extinction efficiency (normalized extinction cross-section) is shown in Fig. 3.

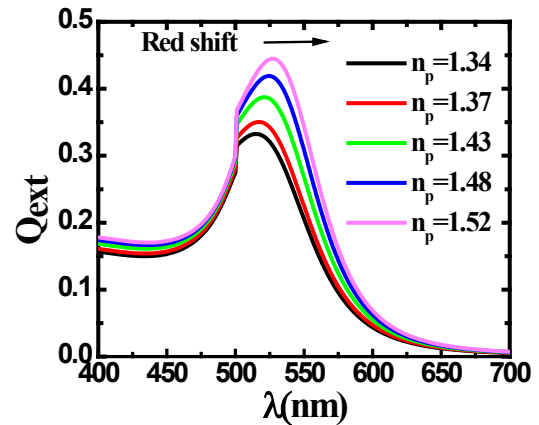


Figure 3. Calculated extinction efficiency (normalized cross-section) for 5 nm gold core coated with responsive PNIPAM outer shell thickness of 2 nm. As the concentration of solvent PNIPAM change with external stimuli there will change in the refractive index leading to red shift in the resonant peak. The surrounding medium refractive index will be 1.33 (water). The optimized linear dependent refractive index of the polymeric shell at 2 nm thick coated in 5nm gold core is taken from ref.[21].

The normalized extinction cross-section (absorption and scattering) at swollen state with optimized refractive index ($n_p=1.34$) is 0.332 with corresponding resonating peak wavelength of 515 nm.

This evidences that the extinction efficiency (scattering and absorption) spectra show a resonant behavior by virtue of occurrence of localized surface plasmon resonance at resonant wavelength (λ_R) = 515 nm, 517 nm, 521 nm and 525 nm for an optimized refractive index of 1.34 ($\chi = 2.0k_B T$), 1.37 ($\chi = 1.2k_B T$), 1.43 ($\chi = 0.8k_B T$), 1.48 ($\chi = 0.0k_B T$), respectively and corresponding magnitudes of extinction efficiency of 0.332, 0.351, 0.38 and 0.41, respectively. It is found that there will be a red shift in the resonant peak with increase in refractive index of polymer shell layer with change in the external physical and chemical environment/stimuli. The variation of resonant peak wavelength as the soft shell evolves from a swollen ($\chi = 2.0k_B T$) to a collapsed state ($\chi = 0.0k_B T$) with optimized refractive index is well suitable for refractive index-based sensing/detection. The performance of the sensor is analyzed through sensing parameters: (I) quality factor (QF) of extinction resonance peak, (II) sensitivity (S) and (III) figure of merit (FOM). The sensitivity (S) of the sensor is calculated as the rate of shift of resonant peak wavelength with the variation in the refractive index (n_p) of shell medium, and the same is mathematically written as [30]:

$$S(\text{nm} / \text{RIU}) = d\lambda_R / dn_p \quad (2)$$

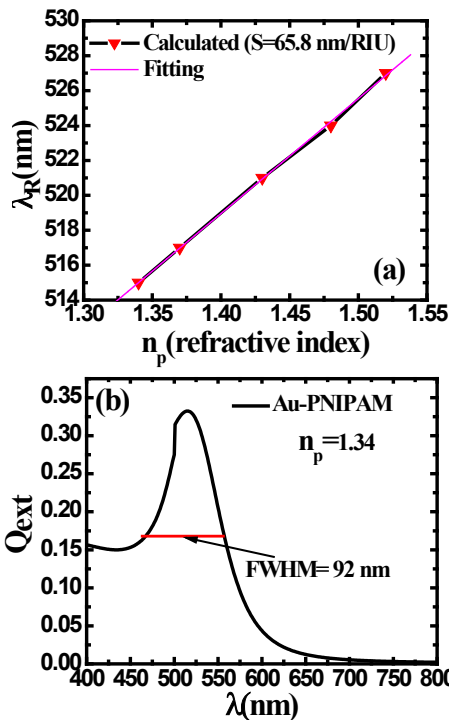


Figure 4. (a) Calculated dependence of the resonant wavelength (λ_R (nm)) on the refractive index (n_p) of the responsive shell medium PNIPAM. (b) Full width half

maximum at the resonant peak is calculated as 92 nm at $n_p = 1.34$ ($\chi = 2.0k_B T$).

The calculated sensitivity (S) using equation 3 is 65.8 nm/RIU, shown in Fig. 4(a). The resonant peak at swollen state ($n_p = 1.34$) is optimized with resonant wavelength (λ_R) 515 nm and the corresponding calculated full width at half maximum (FWHM) is 92 nm, shown in Fig. 4(b). The quality factor of the resonant peak is calculated as the ratio of resonant wavelength of peak to the full width at half maximum of the resonant peak as [30]:

$$QF = \frac{\lambda_R}{FWHM} \quad (3)$$

This suggests that the resonant peak with smaller full width half maximum corresponds to a higher quality factor of the sensor. The figure of merit (FOM) is defined in terms of quality factor of the extinction resonant peak and the corresponding sensitivity. It is a comprehensive parameter to evaluate the performance of a plasmonic sensor, expressed as [30]:

$$FOM(\text{RIU} / \text{nm}) = QF \times S \quad (4)$$

The calculated figure of merit (FOM) using equation 4 is $\sim 3.6 \times 10^2 \text{ RIU/nm}$. Overall, the present work suggests that the responsive polymer-based plasmonic system provides an efficient refractive index-based sensing mechanism for external physical and chemical stimuli.

SUMMARY

In this work we assessed the bio/chemical sensing characteristics of an Au-coated PNIPAM-based plasmonic nano system. The theoretically estimated sensitivity (S) in the present work is 65.8 nm/RIU and the optimized figure of merit is $\sim 3.6 \times 10^2 \text{ RIU/nm}$. It is evident that bio/chemical sensors with high sensitivity and figure of merit can be developed by employing plasmonic modes in an Au-PNIPAM based system. The availability of hybrid responsive polymer-based plasmonic nanosystem can open the door for advanced applications.

Acknowledgement: Sumit Faujdar gratefully acknowledges the Department of Science and Technology (DST), Government of India for providing financial support through inspire fellowship (Code no. IF210244).

REFERENCES

1. N. Jiang, X. Zhuo, J. Wang, *Chem. Rev.*, **118**, 3054 (2018).
2. R. P. Feynman, *Engineering and Science*, **5**, 22 (1960).

3. W. L. Barnes, A. Dereux, T. W. Ebbesen, *Nature*, **424**, 824 (2003).
4. E. Ozbay, *Science*, **311**, 189 (2006).
5. M. S. Shishodia, P. V. V. Jayaweera, S. G. Matsik, A. G. U. Perera, H. C. Liu, M. Buchanan, *Photonics and Nanostructures: Fundam. Appl.*, **9**, 95 (2011).
6. P. Pathania, M. S. Shishodia, *Plasmonics*, **16**, 2717 (2021).
7. P. Pathania, M. S. Shishodia, *Plasmonics*, **14**, 1435 (2019).
8. M. S. Shishodia, P. Pathania, *Phys. Plasmas*, **25**, 042101 (2018).
9. S. Faujdar, P. Pathania, *Materials Today: Proceedings*, **57**, 2295 (2022).
10. M. S. Shishodia, A. G. U. Perera, *J. Appl. Phys.* **109**, 043108 (2011).
11. J. Katyal, R. Soni, *Plasmonics*, **9**, 1171(2014).
12. R. D. Averitt, S. L. Westcott, N. J. Halas, *JOSA A*, **16**, 10 (1999).
13. K. Tanabe, *J. Phys. Chem.*, **C112**, 15721 (2008).
14. Tao Ding, J. J. Baumberg, *Nanoscale Adv.*, **2**, 1410 (2020).
15. J. F. Herrmann, F. Kretschmer, S. Höppener, C. Höppener, U. S. Schubert, *Small*, **13**, 39 (2017).
16. J.-W. Jeon, J. Zhou, J. A. Geldmeier, J. F. Ponder, Jr., M. A. Mahmoud, M. El-Sayed, J. R. Reynolds, V. V. Tsukruk, *Chem. Mater.* **28**, 7551 (2016)
17. S. Wu, L. Lei, Y. Xia, S. Oliver, Y. Xia, X. Chen, C. Boyer, Z. Nie, S. Shi, *Polym. Chem.*, **12**, 6903 (2021).
18. M. M. Miller, A. A. Lazarides, *J. Phys. Chem. B*, **109**, 21556 (2005).
19. R. S. Lee, Y. T. Huang, W. H. Chen, *J. Appl. Polym. Sci.*, **118**, 1634 (2010).
20. E. S. Gill, S. M. Hudson, *Prog. Polym. Sci.* **29**, 1173 (2004).
21. M. Tagliazucchi, M. G. Blaber, G. C. Schatz, E. A. Weiss, I. Szleifer, *ACS Nano*, **6**, 8397 (2012).
22. F. D Jochum, P. Theato, *Chem. Commun.*, **46**, 6717 (2010).
23. M. Emamzadeh, G. Pasparakis, *Sci. Rep.*, **11**, 9404 (2021).
24. A. Pakravan, M. Azizi, F. Rahimi, F. Bani, F. Mahmoudzadeh, R. Salehi, M. Mahkam, *Cancer Nanotechnology*, **12**, 1 (2021).
25. B. Jeon, A. Gutowska, *Trends in Biotechnology*, **20**, 305 (2002).
26. N. Carl, J. Sindram, M. Gallei, S. U. Egelhaaf, M. Karg, *Phys. Rev. E.*, **100**, 052605 (2019).
27. F. Diehl, S. Hageneder, S. Fossati, S. K. Auer, J. Dostalek, U. Jonasl, *Chem. Soc. Rev.*, **51**, 3926 (2022).
28. A. Choe, J. Yeom, R. Shanker, M. P. Kim, S. Kang, H. Ko, *NPG Asia Mater.*, **10**, 912 (2018).
29. C. F. Bohren, D. R. Huffman, Wiley, New York, 1983.
30. Y. Tao, Z. Guo, A. Zhang, J. Zhang, B. Wang, S. Qu, *Opt. Commun.*, **349**, 193 (2015).